

AN EFFICIENT \mathcal{Q} -TENSOR-BASED ALGORITHM FOR LIQUID CRYSTAL ALIGNMENT AWAY FROM DEFECTS*

K. R. DALY[†], G. D’ALESSANDRO[†], AND M. KACZMAREK[‡]

Abstract. We develop a fast and accurate approximation of the normally stiff equations which minimize the Landau–de Gennes free energy of a nematic liquid crystal. The resulting equations are suitable for all configurations in which defects are not present, making them ideal for device simulation. Specifically they offer an increase in computational efficiency by a factor of 100 while maintaining an error of order (10^{-4}) when compared to the full stiff equations. As this approximation is based on a \mathcal{Q} -tensor formalism, the sign reversal symmetry of the liquid crystal is respected. In this paper we derive these equations for a simple two-dimensional case, where the director is restricted to a plane, and also for the full three-dimensional case. An approximation of the error in the perturbation scheme is derived in terms of the first order correction, and a comparison to the full stiff equations is given.

Key words. \mathcal{Q} -tensor, nematic liquid crystals, alignment, approximation methods, numerical methods

AMS subject classifications. 35Q99, 35B38, 82D30, 58Z05

DOI. 10.1137/100796467

1. Introduction. The modeling and simulation of liquid crystals for device purposes is an active area of research with a wide variety of applications [1, 14]. In most applications macroscopic continuum models are used to determine liquid crystal alignment under the influence of an applied electric or magnetic field. There are two main approaches to continuum modeling. The Frank–Oseen (FO) model [8, 20] describes the liquid crystal in terms of a unit vector $\hat{\mathbf{n}}$, also referred to as the director. This model is computationally very efficient. However, although the vector representation of the liquid crystal may be considered quite intuitive, it is physically incorrect as it does not respect the inversion symmetry of the liquid crystal; i.e., $\hat{\mathbf{n}}$ and $-\hat{\mathbf{n}}$ represent the same state of the liquid crystal. This limits the application of the FO model to geometries in which the liquid crystal orientation angle is bounded between 0 and $\pi/2$. Further, the microscopic order of the nematic phase, which depends on temperature, is not considered. This makes the model unsuitable for geometries in which defects, nonsmooth variations in $\hat{\mathbf{n}}$, can occur.

To overcome these problems an approach was developed by de Gennes in which the liquid crystal alignment is represented by a tensor, \mathcal{Q} , which is proportional to $\hat{\mathbf{n}} \otimes \hat{\mathbf{n}}$ [7]. This tensor is invariant with respect to the transformation $\hat{\mathbf{n}} \rightarrow -\hat{\mathbf{n}}$. Further, this theory takes into account the orientational order of the liquid crystal through the temperature-dependent bulk energy, sometimes referred to as the thermotropic energy, and can therefore be used to describe situations in which sharp variations in the liquid crystal alignment—otherwise known as defects—occur. The main disadvantage of this method is that, due to the difference in time scales between the thermotropic

*Received by the editors May 25, 2010; accepted for publication June 28, 2010; published electronically September 16, 2010.

<http://www.siam.org/journals/siap/70-8/79646.html>

[†]School of Mathematics, University of Southampton, Southampton SO17 1BJ, UK (krd103@soton.ac.uk, dales@soton.ac.uk).

[‡]School of Physics, University of Southampton, Southampton SO17 1BJ, UK (M.Kaczmarek@soton.ac.uk).

and elastic properties of the liquid crystals, the final equations are numerically stiff, making computation expensive.

Often the advantages of using a \mathcal{Q} -tensor model outweigh the disadvantage of increased computation time. However, there are devices, such as photorefractive cells [6] or spatial light modulators [19], in which the FO model is inappropriate as the liquid crystals may rotate in an unbounded way. However, as there are no defects in these cells, the Landau–de Gennes \mathcal{Q} -tensor model is unnecessarily expensive to compute.

Numerical methods to overcome the stiffness of the full \mathcal{Q} -tensor equations include the scaling of the elastic and electrostatic coefficients [25] and the renormalization of the liquid crystal director after each time step [11]. Codes also exist which solve the full stiff equations. These are usually based around finite element simulations with adaptive meshing techniques to eliminate the need for dense grids away from defects [12, 27].

Although the separation in scales makes the \mathcal{Q} -tensor equations computationally expensive, the small parameters involved can be used to our advantage. Here we use a multiple scales expansion technique to separate the two timescales. On the timescale of interest, i.e., the slow reorientation time of the liquid crystal, the fast timescale equations, which determine the order parameter, can be considered as having reached equilibrium. The resulting equations for the slow timescale are nonstiff and can be solved in a fraction of the time of the full equations. This approximation reduces the computation time by a factor of approximately one hundred and is suitable for any geometry in which the variation in the scalar order parameter may be assumed to be small.

The paper is arranged as follows: In section 2 we introduce the equations governing the free energy of the liquid crystal and make an analogy between our approximation method and the Signorini method originally developed in elasticity [2, 10, 21]. In section 3, to illustrate the method, we derive a simplified two-dimensional model for the case where liquid crystal alignment is restricted to a plane. Equations for alignment are given and an estimate of the accuracy of the method is derived. In section 4 we apply the ideas and methods used in the two-dimensional case to derive equations for the three-dimensional case. A method to approximate the error is also given. Finally section 5 details comparison with the FO and \mathcal{Q} -tensor models that show that the approximation we derive is both fast and accurate.

2. Free energy. We consider the dimensional liquid crystal free energy of the form $\tilde{\mathcal{F}} = \tilde{\mathcal{F}}_e(\tilde{\mathcal{Q}}) + \tilde{\mathcal{F}}_d(\tilde{\mathcal{Q}}) + \tilde{\mathcal{F}}_t(\tilde{\mathcal{Q}})$, where $\tilde{\mathcal{F}}_e$, $\tilde{\mathcal{F}}_d$, and $\tilde{\mathcal{F}}_t$ are, respectively, the electrostatic, elastic, and bulk free energies. The general form of the biaxial liquid crystal alignment tensor, $\tilde{\mathcal{Q}}$, written in terms of the orthogonal unit directors $\hat{\mathbf{n}}$ and $\hat{\mathbf{m}}$, which define the major and minor crystal axes, respectively, is

$$(2.1) \quad \tilde{\mathcal{Q}} = \sqrt{\frac{3}{2}} \tilde{S} \left(\overline{\hat{\mathbf{n}} \otimes \hat{\mathbf{n}}} \right) + \sqrt{\frac{3}{2}} \tilde{\beta} \left(\overline{\hat{\mathbf{m}} \otimes \hat{\mathbf{m}}} \right),$$

where \tilde{S} is the scalar order parameter, $\tilde{\beta}$ is the biaxiality parameter, I is the identity matrix, and $\overline{\hat{\mathbf{n}} \otimes \hat{\mathbf{n}}} = (\hat{\mathbf{n}} \otimes \hat{\mathbf{n}} - 1/3I)$ denotes a traceless symmetric tensor. The total free energy may be obtained by integrating over the cell volume. In the absence of external forces, such as electromagnetic fields or boundaries, this free energy reduces to just the elastic and thermotropic free energies which are $SO(3)$ invariant. Much work has been done to obtain comprehensive expressions for the thermotropic and elastic free energies. Details, including a full derivation of all possible $SO(3)$ invariants up to powers of $\tilde{\mathcal{Q}}^4$, can be found in [13, 15, 16].

Throughout the remainder of this paper we shall assume the simplest possible expressions for these free energies. It should be noted, however, that this restriction is not a necessary condition for this method to work; rather it is a simplification used to clarify the derivation.

The elastic free energy in its simplest form is derived using the one elastic constant approximation. This can be written as

$$(2.2) \quad \tilde{\mathcal{F}}_d = \frac{L}{2} \left| \nabla \tilde{\mathcal{Q}} \right|^2,$$

where L is defined as $L = K/(3\tilde{S}^2)$ and K is the liquid crystal elastic constant. The electrostatic free energy of the liquid crystal takes the form

$$(2.3) \quad \tilde{\mathcal{F}}_e = -\frac{1}{3}\epsilon_0\Delta\epsilon\text{Tr}\left(\tilde{\mathcal{Q}}\tilde{\mathcal{E}}\right),$$

where

$$(2.4) \quad \tilde{\mathcal{E}} = \sqrt{\frac{3}{2}} \overline{\mathbf{E} \otimes \mathbf{E}},$$

ϵ_0 is the permittivity of free space, $\Delta\epsilon$ is the anisotropic relative permittivity, and the electric field is denoted $\tilde{\mathbf{E}} = -\nabla\tilde{\psi}$, where $\tilde{\psi}$ is the electric potential. The effect of temperature on the liquid crystal alignment is described by the bulk free energy, written in terms of a Landau power series expansion of $\tilde{\mathcal{Q}}$ [7] with $SO(3)$ invariance,

$$(2.5) \quad \tilde{\mathcal{F}}_t = \frac{1}{2}A(T - T^*)\text{Tr}\left(\tilde{\mathcal{Q}}^2\right) - \sqrt{6}B\text{Tr}\left(\tilde{\mathcal{Q}}^3\right) + \frac{1}{2}C\text{Tr}^2\left(\tilde{\mathcal{Q}}^2\right),$$

where A , B , and C are the bulk thermotropic coefficients which are assumed to be independent of temperature. The temperature dependence of this energy is described entirely by $T - T^*$, where T^* is the pseudocritical temperature at which the isotropic phase becomes unstable.

To ensure the traceless symmetric properties of our $\tilde{\mathcal{Q}}$ and $\tilde{\mathcal{E}}$ are respected, we express the free energy on the basis of traceless symmetric tensors [22],

$$\tilde{\mathcal{Q}} = \sum_{p=1}^5 \tilde{a}_p T^{(p)} \quad \text{and} \quad \tilde{\mathcal{E}} = \sum_{p=1}^5 \tilde{e}_p T^{(p)},$$

where

$$(2.6) \quad \begin{aligned} T^{(1)} &= \frac{1}{\sqrt{6}} (-\mathbf{e}_x \otimes \mathbf{e}_x - \mathbf{e}_y \otimes \mathbf{e}_y + 2\mathbf{e}_z \otimes \mathbf{e}_z), \\ T^{(2)} &= \frac{1}{\sqrt{2}} (\mathbf{e}_x \otimes \mathbf{e}_x - \mathbf{e}_y \otimes \mathbf{e}_y), \quad T^{(3)} = \frac{1}{\sqrt{2}} (\mathbf{e}_x \otimes \mathbf{e}_y + \mathbf{e}_y \otimes \mathbf{e}_x), \\ T^{(4)} &= \frac{1}{\sqrt{2}} (\mathbf{e}_x \otimes \mathbf{e}_z + \mathbf{e}_z \otimes \mathbf{e}_x), \quad T^{(5)} = \frac{1}{\sqrt{2}} (\mathbf{e}_y \otimes \mathbf{e}_z + \mathbf{e}_z \otimes \mathbf{e}_y). \end{aligned}$$

We rescale the order parameter $S = \frac{3C}{2B}\tilde{S}$, the biaxiality parameter $\beta = \frac{3C}{2B}\tilde{\beta}$, the tensor field $\mathcal{Q} = \frac{3C}{2B}\tilde{\mathcal{Q}}$, and the component fields $a_p = \frac{3C}{2B}\tilde{a}_p$ and $e_p = \tilde{e}_p/\psi_0^2$, where ψ_0 is a typical potential, $\psi = \tilde{\psi}/\psi_0$. For compactness of notation, from now on we adopt the convention of summing over repeated indices, unless stated otherwise.

We also indicate with \mathbf{a} and \mathbf{e} the vectors with components a_p and e_p . Finally we nondimensionalize to obtain the scaled free energy,

$$(2.7) \quad \mathcal{F} = \frac{\xi_0^2}{2} |\nabla \mathbf{a}|^2 - \chi_a \mathbf{a} \cdot \mathbf{e} + \frac{T_0}{2} |\mathbf{a}|^2 + \frac{1}{2} |\mathbf{a}|^4 - \sqrt{6} \sum_{p,q,r} \text{Tr} \left(T^{(p)} T^{(q)} T^{(r)} \right) a_p a_q a_r.$$

The nondimensional elastic constant ξ_0^2 , the electrostatic coefficient χ_a , and the scaled temperature T_0 are

$$\xi_0^2 = \frac{9C}{2B^2} \frac{L}{L_x^2}, \quad \chi_a = \frac{9\epsilon_0 \Delta \epsilon C^2}{2L_x^2 B^3} \psi_0^2, \quad T_0 = \frac{T - T^*}{T_c - T^*},$$

where T_c is the clearing point temperature and L_x is the characteristic length of the geometry studied. We have rescaled space so that $(\hat{x}, \hat{z}) = (x, z)/L_x$. Typically $T_0 \sim O(1)$, while $\xi_0^2 \sim O(10^{-7})$ and $\chi_a \sim O(10^{-6})$.

The separation in scales between the various terms in the free energy cause the Euler–Lagrange equations, which minimize (2.7), to be stiff. As a result the computing times required for even relatively simple geometries become very large. In situations where the elastic and electrostatic free energies remain small we can initially consider only the critical points of the bulk free energy. The elastic and electrostatic free energies can then be considered as a perturbation. It is this assumption that makes this method inappropriate for defect modeling.

2.1. Critical points under slightly broken symmetry. Before we consider the case of the liquid crystal it is useful to consider a general free energy of the type given in (2.7). The free energy $\mathcal{F}(\mathbf{a})$ consists of a symmetric bulk free energy perturbed by a small symmetry breaking contribution from the elastic and electrostatic energies. We denote these terms $\mathcal{F}_t(\mathbf{a})$ and $\mathcal{L}(\mathbf{a})$, respectively, where $\mathcal{L}(\mathbf{a})$, $\mathcal{F}_t(\mathbf{a}) \in \mathbb{R}^5$ in the three-dimensional case and $\mathcal{L}(\mathbf{a})$, $\mathcal{F}_t(\mathbf{a}) \in \mathbb{R}^2$ in the two-dimensional case. For simplicity we consider here the case that $\mathcal{L}(\mathbf{a})$ has only the electrostatic energy component, so that the liquid crystal state is described by a single five-dimensional vector \mathbf{a} , rather than a five-component vector field $\mathbf{a}(\mathbf{x})$. This allows us to describe the perturbation scheme in very general terms as the effect of a symmetry-breaking perturbation on an invariant manifold of solutions of a set of ordinary differential equations. In the more general case where the elastic energy is also considered we would have to deal with partial differential equations for vector fields; however, we expect that the main ideas outlined here would remain valid.

As the bulk energy is $SO(3)$ invariant the critical points of $\mathcal{F}_t(\mathbf{a})$ will form an orbit of solutions in the five-dimensional component space. Specifically, for the general case corresponding to a biaxial minimizer, the group orbit will be a 3-manifold, while in the special case corresponding to uniaxial minimizers the orbit reduces to a 2-manifold.

The effect of the first order perturbation $\mathcal{L}(\mathbf{a})$ is to break the symmetry and to collapse the invariant manifold of critical points to a smaller set near the manifold. This setting is very similar to the Signorini perturbation scheme, originally derived in the context of elastostatics [2, 10, 21, 26], but of wider potential application [3]. This scheme determines the equilibrium configuration of an elastic body under the effect of applied stresses using a perturbation expansion in powers of the applied stress. In the context of liquid crystals, the role of the “applied stresses” is played by the (small) elastic and electrostatic forces, and our approximation is the first step of a standard Signorini expansion.

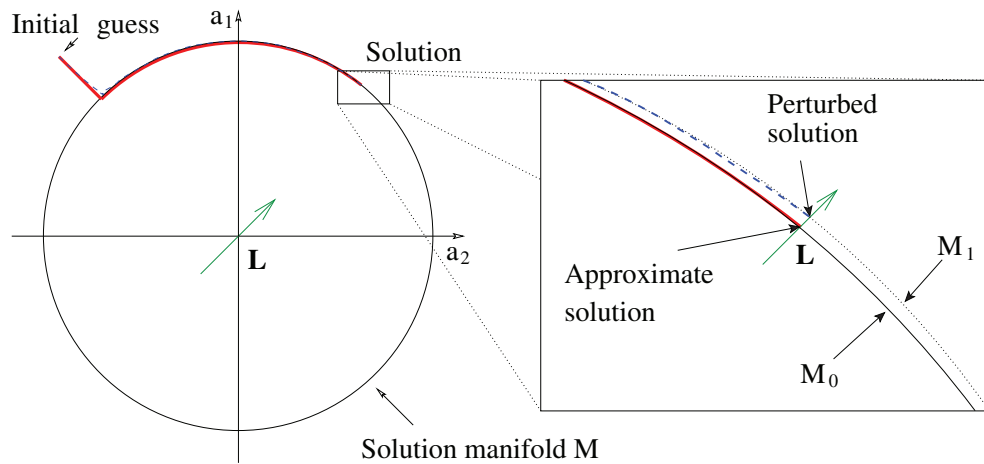


FIG. 1. Graphical representation of the Signorini perturbation scheme. For some initial point in the phase space (a_1, a_2) there is rapid convergence at a rate τ_0 to the solution manifold. Motion along the manifold, driven by the flow \mathbf{L} , occurs much more slowly at a rate τ_1 . The critical point on M_0 is found when \mathbf{L} is orthogonal to $T_{\mathbf{a}}$. As M_0 is close to M_1 the solution can be approximated by the point on M_0 whose surface normal intersects M_1 close to the perturbed solution.

We consider an orbit M_0 consisting of the critical points of the bulk energy $\mathcal{F}_t(\mathbf{a})$ with tangent space $T_{\mathbf{a}}M_0$ at $\mathbf{a} \in M_0$. As M_0 consists entirely of critical points, then $T_{\mathbf{a}}M_0 \subset \ker(\mathcal{H})$, where \mathcal{H} is the Hessian of the bulk free energy. If the critical points of the bulk free energy are nondegenerate in the direction normal to the manifold, then the tangent space coincides with the kernel, $T_{\mathbf{a}}M_0 = \ker(\mathcal{H})$. Therefore, M_0 is a normally hyperbolic invariant manifold for the flow, $-\nabla_{\mathbf{a}}\mathcal{F}_t(\mathbf{a})$, where $\nabla_{\mathbf{a}}$ denotes differentiation with respect to the components of the vector \mathbf{a} .

The effects of the perturbative terms can be understood by the invariant manifold theory. If the perturbed flow, $-\nabla_{\mathbf{a}}(\mathcal{F}_t + \mathcal{L})$, and its first derivative are sufficiently close to the unperturbed flow, then there exists a smooth invariant manifold M_1 close to M_0 . The behavior of the perturbed flow along M_1 will be comparable to the flow restricted to M_0 [26]. Specifically, a point p_0 on M_0 will correspond to a point p_1 on M_1 , where p_1 is the intersection of the normal to M_0 at p_0 and M_1 . If all nonzero eigenvalues of \mathcal{H} are positive, then the dynamical behavior of the flow close to the manifold will consist of exponential attraction towards the manifold followed by a slow drift along it [9].

As the perturbation $-\nabla_{\mathbf{a}}(\mathcal{F}_t + \mathcal{L})$ is also a gradient vector field, then the local minima on M_1 will be attracting stationary points. For nondegenerate critical points these are in 1 : 1 correspondence with the local minima of the perturbed function restricted to the unperturbed manifold M_0 . The critical points restricted to M_0 are found when the flow $\mathbf{L} = -\nabla_{\mathbf{a}}\mathcal{L}$ is orthogonal to $T_{\mathbf{a}}$. This is represented graphically for the simplified two-dimensional case in Figure 1.

In the simple two-dimensional case considered in section 3 the symmetry group is $SO(2)$ under the action of rotation on \mathbb{R}^2 . In this case there will be two critical points on the perturbed manifold. These correspond to an unstable maximum and a stable minimum.

In the three-dimensional case (see section 4), the situation is more complicated. The bulk energy minimizers form an orbit of the conjugacy action of $SO(3)$ on the

five-dimensional space of traceless symmetric matrices (see section 4.2). This orbit is parametrized locally by the direction of the major axis of the liquid crystal molecule (two dimensions) together with a circle corresponding to the orientation of the minor axis. For uniaxial minimizers of the bulk free energy, these circles of critical points shrink to radius 0. The result is that liquid crystal orientation can be determined only in terms of the major axis. To determine the orientation of the minor axis in cases where the perturbation induces biaxiality, a further step in the expansion is required.

3. Two-dimensional case. As an example to illustrate the approximation method it is helpful to look at a simplified two-dimensional case where the liquid crystal director is restricted to the x, z plane. The alignment tensor is a 2×2 uniaxial tensor,

$$(3.1) \quad \mathcal{Q}_{ij} = \sqrt{2}S \left(\hat{n}_i \hat{n}_j - \frac{1}{2} \delta_{ij} \right).$$

We can proceed exactly as in section 2 with the simplified basis set of 2×2 traceless symmetric tensors:

$$(3.2) \quad T_1 = \frac{1}{\sqrt{2}} \begin{pmatrix} -1 & 0 \\ 0 & 1 \end{pmatrix}, \quad T_2 = \frac{1}{\sqrt{2}} \begin{pmatrix} 0 & 1 \\ 1 & 0 \end{pmatrix}.$$

Hence

$$\mathcal{Q} = \sum_{p=1}^2 a_p T^{(p)}.$$

In this notation the scalar order parameter is $S^2 = \text{Tr}(\mathcal{Q}^2) = a_1^2 + a_2^2$. The Euler-Lagrange equations of motion, derived using the simplest form of the free energy, are

$$(3.3) \quad \partial_\tau a_n = \xi_0^2 \nabla^2 a_n - T_0 a_n - 2a_n (a_1^2 + a_2^2) + \chi_a e_n,$$

where $n = 1, 2$, $\tau = t/\tau_d$, $\tau_d = [9C/(2B^2)] \zeta$, and the viscosity, ζ , is related to Leslie's rotational viscosity γ_1 by $\zeta = \gamma_1/(3\tilde{S}^2)$.

3.1. Invariant manifold. Due to the smallness of ξ_0^2 and χ_a , equation (3.3) can be seen to have two different timescales. Taking $\eta = \xi_0^2$ as the small parameter, we can write the time derivatives in (3.3) as $\partial_\tau = \partial_{\tau_0} + \eta \partial_{\tau_1}$. Substituting into (3.3) gives

$$(3.4) \quad \partial_{\tau_0} a_n + \eta \partial_{\tau_1} a_n = \eta \nabla^2 a_n - T_0 a_n - 2a_n (a_1^2 + a_2^2) + \eta \chi_0 e_n,$$

where $\chi_0 = \chi_a/\xi_0^2$ is $O(1)$. Observing that only the bulk free energy changes on the fast timescale, we assume that this scale determines only the scalar order parameter. As we are interested only in the slow timescale, i.e., the timescale over which the liquid crystal aligns, we can make the assumption that the fast timescale behavior has reached equilibrium, i.e., $\partial_{\tau_0} = 0$. The slow scale behavior, which is present due to the small elastic and electrostatic terms, will be obtained from the first order correction.

To proceed the component representation of the liquid crystal is rewritten as a power series expansion in η :

$$(3.5) \quad a_n = a_{n,0} + \eta a_{n,1} + O(\eta^2),$$

where $a_{n,j}$ is the n th component of j th order. Substituting into (3.4) and retaining terms only to $O(\eta^0)$ allows us to write

$$(3.6) \quad [T_0 + 2(a_{1,0}^2 + a_{2,0}^2)] a_n = 0,$$

which is satisfied if $(a_{1,0}^2 + a_{2,0}^2) = -T_0/2$. As $S^2 = a_1^2 + a_2^2$, equation (3.6) defines the leading order approximation to the scalar order parameter,

$$(3.7) \quad S_0^2 = -T_0/2.$$

This equation can also be derived by minimizing the corresponding Landau–de Gennes free energy in terms of the scalar order parameter. As described in section 2.1, (3.7) defines a manifold of critical points in the component space $(a_{1,0}, a_{2,0})$. For uniaxial liquid crystals the critical points of the free energy are nondegenerate as $T_0 < 0$. We consider the effects of the elastic and electrostatic free energies as a symmetry-breaking perturbation. In the context of the Signorini expansion this defines the flow along the manifold with, in this case, a single unique minimum, found using the first step of the Signorini expansion.

3.2. Kernel of adjoint (tangent space). This minimum, and hence the liquid crystal alignment, can be found from the first order expansion of (3.3). Retaining terms to $O(\eta)$ and using (3.6) we obtain

$$(3.8) \quad 4 \begin{pmatrix} a_{1,0}^2 & a_{1,0}a_{2,0} \\ a_{1,0}a_{2,0} & a_{2,0}^2 \end{pmatrix} \begin{pmatrix} a_{1,1} \\ a_{2,1} \end{pmatrix} = \begin{pmatrix} \nabla^2 a_{1,0} + \chi_0 e_1 - \partial_{\tau_1} a_{1,0} \\ \nabla^2 a_{2,0} + \chi_0 e_2 - \partial_{\tau_1} a_{2,0} \end{pmatrix}.$$

This is a system of linear equations for $a_{n,1}$ that can be written as $\mathcal{H}\mathbf{a}_1 = \mathbf{L}$. Recall that \mathcal{H} is the Hessian of the bulk free energy. However, in this case this equation has no unique solution as $\det(\mathcal{H}) = 0$. The Hessian is a symmetric real valued function, and therefore $\mathcal{H}^\dagger = \mathcal{H}$, where \mathcal{H}^\dagger denotes the adjoint of \mathcal{H} . Therefore, as stated in section 2.1, for a nontrivial solution to exist, $\mathbf{L} \cdot \ker(\mathcal{H}) = 0$. As this is a two-dimensional system, the kernel of \mathcal{H} is a single vector \mathbf{V} . This gives us the solvability condition $\mathbf{L} \cdot \mathbf{V} = 0$, where $\mathbf{V} = (-a_{2,0}, a_{1,0})^T$ is the eigenvector of zero eigenvalue of \mathcal{H} .

Using the solvability condition, $\mathbf{L} \cdot \mathbf{V} = 0$, we obtain the following equation for $a_{1,0}$ and $a_{2,0}$:

$$(3.9) \quad a_{1,0}\partial_{\tau_1} a_{2,0} - a_{2,0}\partial_{\tau_1} a_{1,0} = a_{1,0}\nabla^2 a_{2,0} - a_{2,0}\nabla^2 a_{1,0} + a_{1,0}\chi_0 e_2 - a_{2,0}\chi_0 e_1.$$

Equation (3.9) can be solved simultaneously with (3.6) to determine the liquid crystal dynamics on the solution manifold.

3.3. Parameterization of the solution. By correctly parameterizing the components $a_{1,0}$ and $a_{2,0}$ we can force the director onto the solution manifold, removing the need to solve the leading order equation. As the leading order solution manifold is $SO(2)$ invariant, we parameterize the solutions in terms of the polar angle $\vartheta \in [0, 2\pi]$. If we write

$$a_{1,0} = S_0 \sin \vartheta \quad \text{and} \quad a_{2,0} = S_0 \cos \vartheta,$$

then (3.7) is automatically satisfied. This representation can be used in (3.9) to determine the time evolution of $a_{n,0}$:

$$(3.10) \quad S_0^2 \frac{\partial a_{n,0}}{\partial \tau_1} = V_n (a_{1,0}\nabla^2 a_{2,0} - a_{2,0}\nabla^2 a_{1,0} + a_{1,0}\chi_0 e_2 - a_{2,0}\chi_0 e_1),$$

where V_n is the n th component of \mathbf{V} . This equation confirms that the motion of the director field is in the direction tangent to the manifold.

Equation (3.10) is an initial value problem for $a_{n,0}$ which can be solved using standard numerical techniques for an initial set of $a_{n,0}$ on the manifold. It is important to note that we need never calculate ϑ , as (3.10) is solved purely in terms of the component representation, $a_{n,0}$. This ensures that the singularities expected in a director model are overcome. It is possible to solve (3.10) for either $n = 1$ or $n = 2$ and calculate $a_{2,0}$ or $a_{1,0}$, respectively, from (3.7). However, this method is not recommended, as computing the square root in (3.7) will introduce a sign ambiguity. The extra computation required to correct this is inefficient and could potentially make the code unstable.

3.4. Order one accuracy check. To determine the accuracy of the expansion, we consider the perturbed manifold M_1 . The equations derived above are suitable only in the case where M_1 is sufficiently close to M_0 .

Physically the minimum distance between the leading order solution and M_1 represents the correction S_1 to the scalar order parameter, $S = S_0 + \eta S_1 + O(\eta^2)$. In general this can be calculated from the singular value decomposition of the $O(\eta)$ equation (3.8). However, in two dimensions the correction can be calculated analytically. After a little algebra we obtain

$$(3.11) \quad S_1 = \frac{1}{\sqrt{-2T_0^3}} [\mathbf{a}_0 \cdot \nabla^2 \mathbf{a}_0 + \chi_0 \mathbf{a}_0 \cdot \mathbf{e}].$$

The magnitude of S_1 can be used to determine the validity of the perturbation expansion. If ηS_1 becomes comparable with S_0 , then the expansion breaks down and the liquid crystal has large variation in order parameter. If this happens, then the full stiff equations (3.3) must be solved.

4. Three-dimensional case. The three-dimensional Euler–Lagrange equations are computed in a similar way to the two-dimensional case:

(4.1a)

$$\eta \frac{\partial a_1}{\partial \tau_1} = \eta (\nabla^2 a_1 + \chi_0 e_1) - T_0 a_1 + 3(a_1^2 - a_2^2 - a_3^2) + \frac{3}{2}(a_4^2 + a_5^2) - 2a_1 \sum_{k=1}^5 a_k^2,$$

(4.1b)

$$\eta \frac{\partial a_2}{\partial \tau_1} = \eta (\nabla^2 a_2 + \chi_0 e_2) - T_0 a_2 - 6a_1 a_2 + \frac{3\sqrt{3}}{2}(a_4^2 - a_5^2) - 2a_2 \sum_{k=1}^5 a_k^2,$$

(4.1c)

$$\eta \frac{\partial a_3}{\partial \tau_1} = \eta (\nabla^2 a_3 + \chi_0 e_3) - T_0 a_3 - 3(2a_1 a_3 - \sqrt{3} a_4 a_5) - 2a_3 \sum_{k=1}^5 a_k^2,$$

(4.1d)

$$\eta \frac{\partial a_4}{\partial \tau_1} = \eta (\nabla^2 a_4 + \chi_0 e_4) - T_0 a_4 + 3a_1 a_4 + 3\sqrt{3}(a_2 a_4 + a_3 a_5) - 2a_4 \sum_{k=1}^5 a_k^2,$$

(4.1e)

$$\eta \frac{\partial a_5}{\partial \tau_1} = \eta (\nabla^2 a_5 + \chi_0 e_5) - T_0 a_5 + 3a_1 a_5 + 3\sqrt{3}(a_3 a_4 - a_2 a_5) - 2a_5 \sum_{k=1}^5 a_k^2,$$

where, as in the two-dimensional case, $\eta = \xi_0^2$ and $\chi_0 = \chi_a/\xi_0^2$. The fast time derivatives have been neglected as, on the timescale of interest, these variations will have reached equilibrium. At this point, for compactness of notation, it is useful to define the first order perturbation L_m in terms of the elastic and electrostatic contributions,

$$(4.2) \quad L_m = \nabla^2 a_{m,0} + \chi e_m - \frac{\partial a_{m,0}}{\partial \tau_1},$$

where $m = 1, \dots, 5$.

4.1. Invariant manifold. In the two-dimensional case the leading order equations are those which minimize the free energy in terms of the scalar order parameter. This minimization fixes the liquid crystal director onto the solution manifold in the two-dimensional space (a_1, a_2) . A similar method can be used in the three-dimensional case using the biaxial \mathcal{Q} -tensor representation (2.1). It can be shown that the stationary points of the leading order free energy function, of the form given in (2.5), are either uniaxial or isotropic [17]. As such the biaxiality parameter β must vanish at leading order. Minimizing the free energy in terms of the scalar order parameter S , as in the two-dimensional case, allows us to obtain the fast timescale equations. The Euler–Lagrange equation of motion that minimizes the leading order scalar order parameter, S_0 , is

$$(4.3) \quad \frac{\partial S_0}{\partial \tau_0} = -2S_0^3 + 3S_0^2 - T_0 S_0,$$

which can be solved for a steady uniaxial state to obtain

$$(4.4) \quad S_0 = \frac{3 + \sqrt{9 - 8T_0}}{4}.$$

Equation (4.4) defines the solution manifold in the five-dimensional component space. The critical points on this manifold are nondegenerate, providing T_0 is below the superheating limit, $T_0 = 9/8$ [18]. In terms of the component representation, the scalar order parameter is given by

$$(4.5) \quad S_0^2 = \sum_{n=1}^5 a_n^2.$$

To fix the biaxiality order parameter to zero, we require

$$(4.6) \quad a_{1,0}^3 + 3a_{1,0}^2(S_0 - a_{1,0}) + \frac{3\sqrt{3}}{2} [a_{2,0}(a_{4,0}^2 - a_{5,0}^2) + 2a_{3,0}a_{4,0}a_{5,0}] = S_0^3.$$

These two equations define a 3-manifold in the five-dimensional component space. However, as the leading order minimizers are uniaxial, there are only two undefined parameters which relate to the angles the liquid crystal makes with the coordinate axes. Therefore, as described in section 2.1, the 3-manifold corresponding to the biaxial stationary points must reduce to a 2-manifold, leading to a degeneracy in the first order correction. Specifically this allows us to determine only the direction of the major crystal axis uniquely.

4.2. Kernel of adjoint (tangent space). As in the two-dimensional case we now need to find the first order correction to the leading order terms which will determine the unique solution on the manifold. Motion across the manifold is determined by the first order perturbation L_m . The first order contribution from the bulk energy is invariant with respect to motion on the leading order manifold. Therefore, for the equation to have a nontrivial solution, we require that the perturbation L_m be orthogonal to the kernel of \mathcal{H} . As $\text{Ker}(\mathcal{H}) = T_a M_0$ the solvability condition is

$$(4.7) \quad L_m \frac{\partial a_{m,0}}{\partial s} = 0,$$

where s parameterizes motion along the tangent space to the manifold. The derivative of $a_{m,0}$ is found by considering the tensor $\mathcal{Q}_{ij}(0)$, which satisfies the perturbed Euler–Lagrange equations. The motion of $\mathcal{Q}_{ij}(0)$ along the manifold by rotation in a spherical coordinate system is defined by the rotation matrix $R_{ij}(s)$, which acts on $\mathcal{Q}_{ij}(0)$ by the conjugacy action $\mathcal{Q}_{ij}(s) = R_{ip}(s)R_{jq}(s)\mathcal{Q}_{pq}(0)$. The rotation matrix $R_{ij}(s)$ is orthogonal, i.e., $R_{ik}(s)R_{jk}(s) = \delta_{ij}$ and $R_{ij}(0) = \delta_{ij}$. Motion along the manifold written in terms of the component representation is

$$(4.8) \quad a_{m,0}(s) = \left[T_{ji}^{(m)} R_{ip}(s) R_{jq}(s) T_{pq}^{(l)} \right] a_{l,0}(0).$$

The derivative of $a_{m,0}$ is found by differentiating (4.8) at $s = 0$:

$$(4.9) \quad \frac{\partial a_{m,0}}{\partial s} = T_{ji}^{(m)} \left[R'_{ip}(0) \delta_{jq} T_{pq}^{(l)} + \delta_{ip} R'_{jq}(0) T_{pq}^{(l)} \right] a_{l,0}(0).$$

To proceed we need to determine $R'_{ij}(0)$; this can be obtained by differentiating the identity $R_{ip}(s)R_{jp}(s) = \delta_{ij}$ at $s = 0$:

$$(4.10) \quad R'_{ip}(0) \delta_{jp} + \delta_{ip} R'_{jp}(0) = 0.$$

For this equation to be satisfied $R'_{ij}(0)$ must be a skewsymmetric tensor expressed on the basis $W^{(n)}$, defined as

$$(4.11) \quad \begin{aligned} W^{(1)} &= \frac{1}{\sqrt{2}} (\mathbf{e}_y \otimes \mathbf{e}_x - \mathbf{e}_x \otimes \mathbf{e}_y), \\ W^{(2)} &= \frac{1}{\sqrt{2}} (\mathbf{e}_x \otimes \mathbf{e}_z - \mathbf{e}_z \otimes \mathbf{e}_x), \\ W^{(3)} &= \frac{1}{\sqrt{2}} (\mathbf{e}_z \otimes \mathbf{e}_y - \mathbf{e}_y \otimes \mathbf{e}_z). \end{aligned}$$

For each $W^{(n)}$ we obtain a different $\partial a_{m,0}/\partial s$ and thus three vectors, $\mathbf{V}^{(n)}$, that span the kernel. The solvability conditions can be written as

$$(4.12) \quad L_m V_m^{(n)} = 0,$$

where the spanning vectors can be explicitly written as

$$(4.13) \quad V_m^{(n)} = T_{ki}^{(m)} \left(T_{ij}^{(p)} W_{jk}^{(n)} - W_{ij}^{(n)} T_{jk}^{(p)} \right) a_{p,0},$$

In terms of the $O(\eta^0)$ components the spanning vectors $\mathbf{V}^{(n)}$ formed by each $W^{(n)}$ are

$$(4.14) \quad \mathbf{V}^{(1)} = \begin{pmatrix} 0 \\ -2a_{3,0} \\ 2a_{2,0} \\ -a_{5,0} \\ a_{4,0} \end{pmatrix}, \quad \mathbf{V}^{(2)} = \begin{pmatrix} -\sqrt{3}a_{4,0} \\ a_{4,0} \\ a_{5,0} \\ \sqrt{3}a_{1,0} - a_{2,0} \\ -a_{3,0} \end{pmatrix}, \quad \mathbf{V}^{(3)} = \begin{pmatrix} \sqrt{3}a_{5,0} \\ a_{5,0} \\ -a_{4,0} \\ a_{3,0} \\ -\sqrt{3}a_{1,0} - a_{2,0} \end{pmatrix}.$$

The first order equations require (4.12) to be satisfied in the direction of each spanning vector. This gives us three equations, one for each of the skewsymmetric tensors $W^{(n)}$. Substituting (4.2) into (4.12), the time-dependent equations are obtained:

$$(4.15) \quad V_m^{(n)} \frac{\partial}{\partial \tau_1} a_{m,0} = V_m^{(n)} \left(\nabla^2 a_{m,0} + \chi e_m \right),$$

where $m = 1, \dots, 5$.

4.3. How to solve equations/parameterization of equations. Equations (4.15) describe the dynamics of the critical point structure on the generic 3-manifold. However, as the bulk minimizers are uniaxial, these 3 equations must reduce to 2 corresponding to the reduction in the dimension of the manifold. Using guidance from the two-dimensional case we exploit the $SO(3)$ invariance of the bulk energy and parameterize the component representation \mathbf{a}_0 in terms of the uniaxial \mathcal{Q} -tensor with principal axis defined by the spherical coordinate angles $[\theta, \phi]$:

$$(4.16) \quad \mathbf{a}_0 = S_0 \begin{pmatrix} 1 - \frac{3}{2} \sin^2 \theta \\ \frac{\sqrt{3}}{2} \sin^2 \theta (2 \cos^2 \phi - 1) \\ \sqrt{3} \sin^2 \theta \cos \phi \sin \phi \\ \sqrt{3} \cos \theta \sin \theta \sin \phi \\ \sqrt{3} \cos \theta \sin \theta \cos \phi \end{pmatrix}.$$

For a free energy which supports biaxial phases the appropriate representation for the component field would be a biaxial tensor expressed in terms of all three Euler angles. Substituting into (4.15), we can simplify the time derivatives to obtain equations for the time derivatives of θ and ϕ :

$$(4.17) \quad 3S_0^2 \frac{\partial \theta}{\partial \tau_1} = \left(\cos \phi V_m^{(2)} - \sin \phi V_m^{(3)} \right) \left(\nabla^2 a_{m,0} + \chi e_m \right),$$

$$3S_0^2 \frac{\partial \phi}{\partial \tau_1} = \frac{1}{\sin^2 \theta} V_m^{(1)} \left(\nabla^2 a_{m,0} + \chi e_m \right).$$

These can be used to describe the time-dependent liquid crystal alignment in all cases except where the liquid crystal is aligned close to the coordinate singularity $\theta = 0, \pi$. If this is the case, then we need to use a multigrid method [23]. We choose a different set of coordinates $(\tilde{\theta}, \tilde{\phi})$, formed by rotating the existing coordinates about the y axis. This second coordinate system produces a set of components which give

time-dependent equations:

$$(4.18) \quad \begin{aligned} 3S_0^2 \frac{\partial \tilde{\theta}}{\partial \tau_1} &= \left(\cos \tilde{\phi} V_m^{(2)} - \sin \tilde{\phi} V_m^{(1)} \right) \left(\nabla^2 a_{m,0} + \chi e_m \right), \\ 3S_0^2 \frac{\partial \tilde{\phi}}{\partial \tau_1} &= -\frac{1}{\sin^2 \tilde{\theta}} V_m^{(3)} \left(\nabla^2 a_{m,0} + \chi e_m \right). \end{aligned}$$

The second coordinate system is singular at $\tilde{\theta} = 0, \pi$, equivalent to $\theta = \pi/2$ and $\phi = 0, \pi$. As such the two coordinate systems cannot be simultaneously singular for a given director. Using the different coordinate systems, the time derivatives of $a_{p,0}$ can be found from the least singular coordinate system as either

$$(4.19a) \quad \frac{\partial a_p}{\partial \tau_1} = V_p^{(1)} \frac{\partial \phi}{\partial \tau_1} - \left(\sin \phi V_p^{(3)} - \cos \phi V_p^{(2)} \right) \frac{\partial \theta}{\partial \tau_1}$$

or

$$(4.19b) \quad \frac{\partial a_p}{\partial \tau_1} = -V_p^{(3)} \frac{\partial \tilde{\phi}}{\partial \tau_1} + \left(\cos \tilde{\phi} V_p^{(2)} - \sin \tilde{\phi} V_p^{(1)} \right) \frac{\partial \tilde{\theta}}{\partial \tau_1}.$$

The strength of the singularity in each coordinate system is determined by the size of θ and $\tilde{\theta}$. This can be directly measured from the size of the x and z components of the director. An appropriate choice of representation, chosen arbitrarily to allow for some overlap between the two, is to use $[\theta, \phi]$ if $|n_z| \leq 4/(3\sqrt{2})$ and $[\tilde{\theta}, \tilde{\phi}]$ if $|n_x| \leq 4/(3\sqrt{2})$. If both of these conditions are satisfied, an average value of $\partial a_p / \partial \tau_1$ obtained from each of the two representations is used.

4.4. Order one accuracy check. As in the two-dimensional case, we wish to determine the correction to the scalar order parameter as an approximation of the accuracy of our method. Unlike the two-dimensional case an analytic expression cannot be obtained. Instead we use the method of singular value decomposition. Given the degenerate $O(\eta)$ equation $\mathcal{H}\mathbf{a}_1 = \mathbf{L}$, we calculate the perturbed manifold M_1 corresponding to the $O(\eta)$ correction to the components \mathbf{a}_1 , where

$$\begin{aligned} \mathcal{H}_{11} &= (4a_{1,0} - 6)a_{1,0} + T_0 + 2 \sum_{n=1}^4 a_{n,0}^2, \\ \mathcal{H}_{22} &= 4a_{2,0}^2 + 6a_{1,0} + T_0 + 2 \sum_{n=1}^4 a_{n,0}^2, \\ \mathcal{H}_{33} &= 4a_{3,0}^2 + 6a_{1,0} + T_0 + 2 \sum_{n=1}^4 a_{n,0}^2, \\ \mathcal{H}_{44} &= 4a_{4,0}^2 - 3a_{1,0} - 3\sqrt{3}a_{2,0} + T_0 + 2 \sum_{n=1}^4 a_{n,0}^2, \\ \mathcal{H}_{55} &= 4a_{5,0}^2 - 3a_{1,0} + 3\sqrt{3}a_{2,0} + T_0 + 2 \sum_{n=1}^4 a_{n,0}^2, \\ \mathcal{H}_{12} &= (6 + 4a_{1,0})a_{2,0}, & \mathcal{H}_{24} &= (4a_{2,0} - 3\sqrt{3})a_{4,0}, \\ \mathcal{H}_{13} &= (6 + 4a_{1,0})a_{3,0}, & \mathcal{H}_{25} &= (4a_{2,0} + 3\sqrt{3})a_{5,0}, \\ \mathcal{H}_{14} &= (4a_{1,0} - 3)a_{4,0}, & \mathcal{H}_{34} &= 4a_{3,0}a_{4,0} - 3\sqrt{3}a_{5,0}, \\ \mathcal{H}_{15} &= (4a_{1,0} - 3)a_{5,0}, & \mathcal{H}_{35} &= 4a_{3,0}a_{5,0} - 3\sqrt{3}a_{4,0}, \\ \mathcal{H}_{23} &= 4a_{2,0}a_{3,0}, & \mathcal{H}_{45} &= 4a_{4,0}a_{5,0} - 3\sqrt{3}a_{3,0}, \end{aligned}$$

and $\mathcal{H}_{ij} = \mathcal{H}_{ji}$. The order parameter correction S_1 is then determined from the components of \mathbf{a}_1 orthogonal to the manifold, $S_1 = \mathbf{a}_0 \cdot \mathbf{a}_1 / S_0$.

TABLE 1

Numerical values of nondimensional constants for a typical photorefractive liquid crystal cell.

$K = 20 \times 10^{-12} \text{N}$	$\epsilon_{\perp} = 4.1$	$\zeta = 0.037 \text{Pa s}$
$A = 0.13 \times 10^6 \text{J K}^{-1} \text{m}^{-3}$	$S = 3.65 \hat{S}$	$\tau_d = 2.56 \times 10^{-7} \text{s}$
$B = 1.6 \times 10^6 \text{Jm}^{-3}$	$L = 6.05 \times 10^{-12} \text{N}$	$\xi_0^2 = 4.39 \times 10^{-7}$
$C = 3.9 \times 10^6 \text{Jm}^{-3}$	$L_x = 12 \times 10^{-6} \text{m}$	$\chi_a = 5.13 \times 10^{-6} \psi_0^2$
$T_0 = -10$	$L_z = 12 \times 10^{-6} \text{m}$	$\chi_I = 3.25 \times 10^{-5} \psi_0^2$
$\epsilon_{\parallel} = 9.1$	$\gamma_1 = 0.081 \text{Pa s}$	$\psi_0 = 1 \text{V}$

5. Examples. To demonstrate the use of the nonstiff approximate liquid crystal equations, we consider a planar cell filled with liquid crystals. A spatially periodic voltage is applied to one boundary, while the other is set to a uniform zero volts. This is a realistic model for a photorefractive liquid crystal cell [6, 4], a device used for optical coupling and as an optically addressable spatial light modulator. This is an interesting device for testing this algorithm as it allows for three-dimensional orientation of the liquid crystal directors and has a simple geometry.

Under appropriate conditions the test geometry is a square in the x, z plane. Periodic conditions are imposed in the x direction such that $\mathbf{a}(x + L_x, z) = \mathbf{a}(x, z)$, and Dirichlet boundary conditions, corresponding to infinite anchoring strength, are imposed at $z = 0$ and $z = L_z$. The liquid crystal is aligned by application of a spatially modulated voltage $\psi(x, L_z) = \psi_a \sin^2(\pi x/L_x)$ at one boundary, where ψ_a is the applied voltage amplitude, while the other is earthed, $\psi(x, 0) = 0$.

First we verify the two-dimensional liquid crystal model derived in section 3. This is done through comparison to the full stiff time-dependent \mathcal{Q} -tensor equations and through comparison to a time-dependent FO model. In this case the director orientation is restricted to the x, z plane by the planar, in plane boundary conditions. As is typical, due to the alignment layers used in these cells, a small pretilt is applied at $z = L_z$. The parameters used in our simulation are given in Table 1. The spatial derivatives are calculated using a pseudospectral method [24] and, for ease of implementation, the time derivative is calculated using the MATLAB multistep solver ODE113. A public domain version of the MATLAB code is available at [5].

The FO model is derived by minimizing the FO free energy [8, 20],

$$(5.1) \quad \tilde{\mathcal{F}}_{FO} = \frac{K}{2} (\nabla \theta_{FO})^2 - \frac{1}{2} \epsilon_0 \epsilon_u (\tilde{\mathbf{E}})^2 - \frac{1}{2} \epsilon_0 \Delta \epsilon (\hat{\mathbf{n}} \cdot \tilde{\mathbf{E}})^2,$$

in terms of the director angle θ_{FO} ,

$$(5.2) \quad \frac{\partial \theta_{FO}}{\partial \tau_{FO}} = \nabla^2 \theta_{FO} + \frac{1}{2} \delta_1 [\sin 2\theta_{FO} (E_x^2 - E_z^2) + 2 \cos 2\theta_{FO} E_x E_z],$$

where $\delta_1 = (\epsilon_0 \Delta \epsilon / K) \psi_0^2$ and $\tau_{FO} = t [K / (L_x^2 \gamma_1)]$. Starting from the same initial conditions, the FO and \mathcal{Q} -tensor models are integrated till steady state is reached. The resulting configurations are compared and the differences are computed.

First we compare the FO model with the approximate \mathcal{Q} -tensor model. We observe that there is an area of the FO model which does not show good agreement with the \mathcal{Q} -tensor model. By plotting the resulting director field as vectors and comparing the numerical gradient, it can be seen that these errors correspond to the points where the FO model predicts unphysical gradients; see Figure 2.

Similarly we can compare the full stiff \mathcal{Q} -tensor equations with the nonstiff approximate equations derived in section 3. Figure 3 shows a plot of the error in the

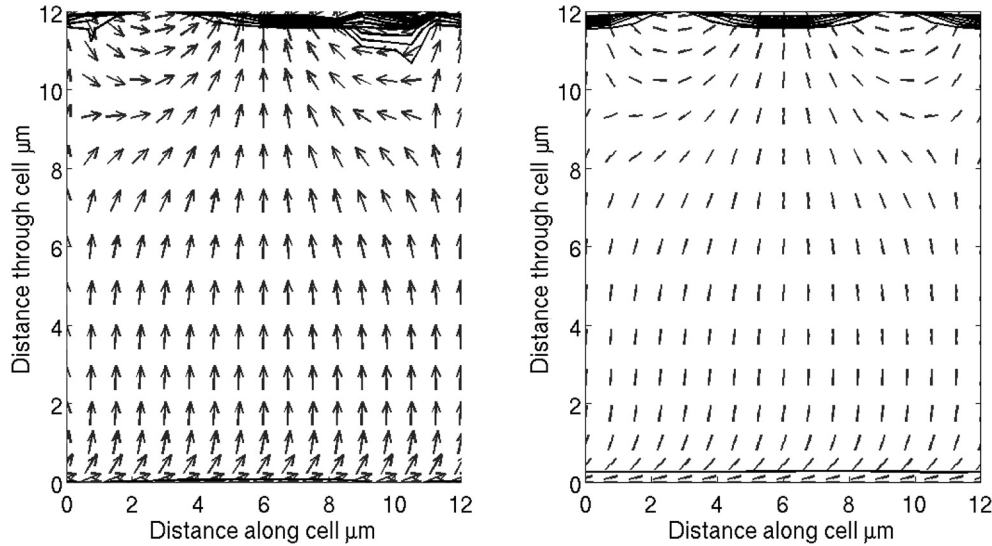


FIG. 2. Comparison of liquid crystal alignment. The left and right images show the director alignment for the FO model and the approximate Q -tensor model, respectively. Director fields for both models are plotted, contour lines show areas of equal elastic energy, $|\nabla\theta_{FO}|^2 = C$ in the FO model, and $|\nabla\mathbf{a}|^2 = C$ in the Landau-de Gennes model. The inaccuracy of the FO model can be seen in the asymmetry of $|\nabla\theta_{FO}|^2$ near the boundary.

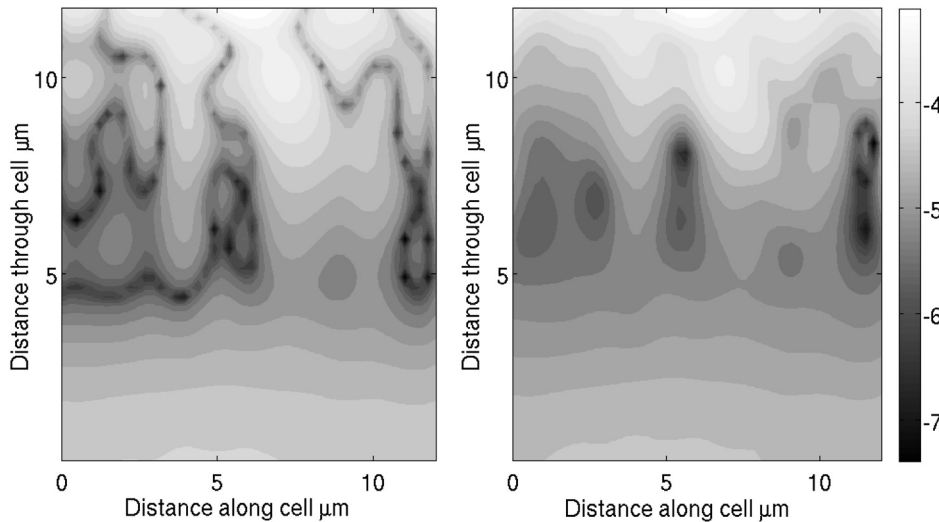


FIG. 3. Two-dimensional director field error calculation for a 10 volt spatially modulated electric field plotted on a logarithmic scale. The liquid crystal has strong planar anchoring boundary conditions at $z = 0$ and $z = L_z$ and periodic boundary conditions in the x direction. The error is calculated both through calculation of the correction to the scalar order parameter S_1/S_0 (left) and through comparison to the full stiff equations δa (right).

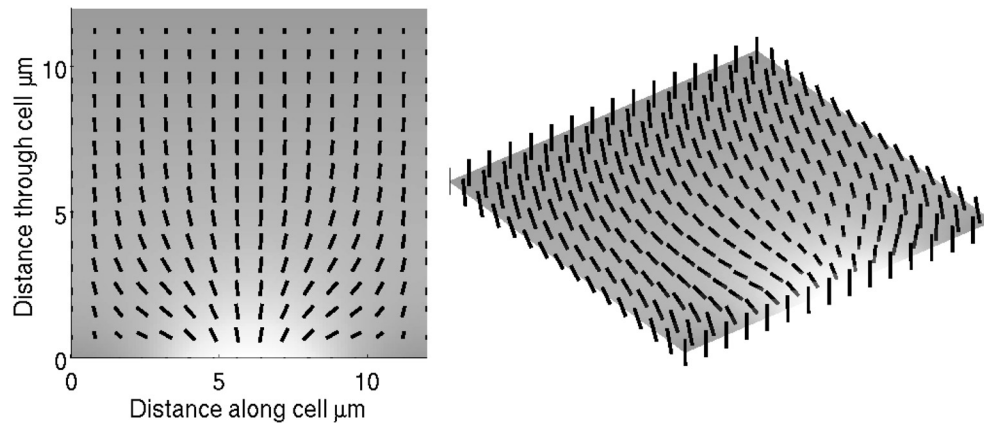


FIG. 4. Typical director field plot calculated using approximate equations for a 5 volt spatially modulated electric field. The shading corresponds to the voltage throughout the cell. The liquid crystal alignment is parallel to the surface but twisted out of plane. This forces full three-dimensional orientation of the liquid crystal when subject to a spatially modulated electric field.

approximate equation calculated using both the first order correction to the order parameter, (3.11), and the difference in the two simulations divided by the leading order scalar order parameter, (3.7),

$$(5.3) \quad \delta a = \frac{1}{S_0} \|\mathbf{a}_{approx} - \mathbf{a}_{stiff}\|.$$

Not only is the error very low, but when the two error plots are compared it can be seen that the approximate error is qualitatively comparable with the difference between the full stiff equations and the approximations derived here. In both plots the error peaks around the points of highest liquid crystal variation. This is expected, as these points correspond to those with highest elastic energy.

Second we compare the three-dimensional model, derived in section 4, with the full stiff \mathcal{Q} -tensor model. In this case the boundary conditions fix the director out of plane in the y direction to allow for full three-dimensional reorientation.

The steady state alignment results are shown in Figure 4. The comparison to the full stiff equations is shown in Figure 5 with error calculated using both the correction to the scalar order parameter, calculated using singular value decomposition, and the percentage error given in (5.3), where S_0 for the three-dimensional case is given in (4.4). Again it can be seen that the difference between the two methods is very low and that the error approximation using the singular value decomposition method is comparable to the true error. We find for the same number of grid points, 12 in each spatial dimension, that the stiff code takes over an hour to converge, while the approximate code converges to a solution with $\delta a \sim O(10^{-4})$ in a time of ≈ 45 seconds.

6. Conclusion. The approximate equations derived in this paper determine the liquid crystal alignment, which minimizes the Landau-de Gennes free energy in the absence of defects. They can be solved in a fraction of the time required to solve the full stiff equations.

We have derived equations for both a two- and three-dimensional case and have implemented both as nonstiff initial value problems in MATLAB. Estimates of the accuracy of these equations have been derived in terms of the first order correction

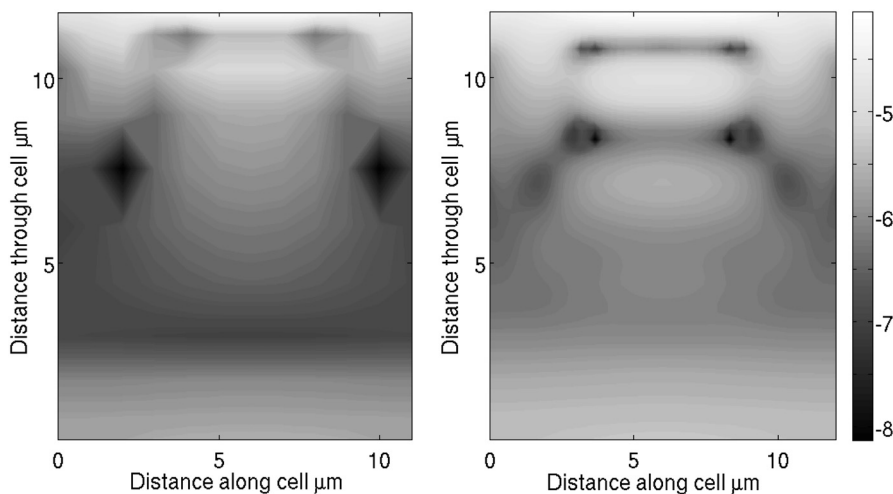


FIG. 5. Three-dimensional director field error calculation for a 5 volt spatially modulated electric field plotted on a logarithmic scale. The liquid crystal has strong out-of-plane anchoring boundary conditions at $z = 0$ and $z = L_z$ and periodic boundary conditions in the x direction. The error is calculated both through calculation of the correction to the scalar order parameter S_1/S_0 (left) and through comparison to the full stiff equations δa (right).

to the component values and have been shown to give strong qualitative agreement with the deviation of the approximation from the full stiff equations.

It should be noted that the free energy functions used in this paper are the simplest possible forms of the free energy. However, generalization to other free energy functions, whose bulk energy minimizers are uniaxial, is relatively straightforward. Generalizing this method to situations where the free energy supports biaxial states is also possible. In this case M_0 is a 3-manifold and expressions must be found for the equations of motion using a biaxial tensor representation with major and minor axes determined using all three Euler angles.

The major advantage of these equations with respect to the full stiff minimizers is that they can be computed in a fraction of the time while producing results with error $\sim O(10^{-4})$. This will be of great importance in medium- to large-scale models where computational efficiency becomes an issue. The assumption that the elastic and electrostatic free energies remain small makes these equations suitable for geometries in which defects do not occur. As such these approximate equations will be of most use in applications where defects are undesirable. This is the case in many optical devices where smooth alignment of the liquid crystal is important, but the FO model predicts nonphysical configurations.

Acknowledgments. The authors would like to thank Dr. David Chillingworth, Dr. Ian Hawke, Prof. Tim Sluckin, and Mr. Richard Slessor for helpful discussions and suggestions.

REFERENCES

- [1] B. BAHADUR, *Liquid Crystals: Applications and Uses*, World Scientific, River Edge, NJ, 1990.
- [2] G. CAPRIZ AND P. PODIO GUIDUGLI, *On Signorini's perturbation method in finite elasticity*, Arch. Rational Mech. Anal., 57 (1974), pp. 1–30.

- [3] D. R. J. CHILLINGWORTH, *The Signorini perturbation scheme in an abstract setting*, Proc. Roy. Soc. Edinburgh Sect. A, 119 (1991), pp. 373–395.
- [4] G. COOK, C. A. WYRES, M. J. DEER, AND D. C. JONES, *Hybrid organic-inorganic photorefractives*, Proc. SPIE, 5213 (2003), pp. 63–77.
- [5] K. R. DALY AND G. D'ALESSANDRO, *Homepage of the Defect Free Q-Tensor Approximation Code*, <http://www.personal.soton.ac.uk/dales/DFQTA/>.
- [6] K. R. DALY, G. D'ALESSANDRO, AND M. KACZMAREK, *Regime independent coupled-wave equations in anisotropic photorefractive media*, Appl. Phys. B Lasers Opt., 95 (2009), pp. 589–596.
- [7] P. G. DE GENNES AND J. PROST, *The Physics of Liquid Crystals*, 2nd ed., Oxford University Press, New York, 1993.
- [8] F. C. FRANK, *On the theory of liquid crystals*, Discuss. Faraday Soc., 25 (1958), pp. 19–28.
- [9] M. GOLUBITSKY AND D. G. SCHAEFFER, *A discussion of symmetry and symmetry breaking*, in Singularities, Part 1 (Arcata, CA, 1981), Proc. Symp. Pure Math. 40, AMS, Providence, RI, 1983, pp. 499–515.
- [10] G. GRIOLI, *Mathematical Theory of Elastic Equilibrium (Recent Results)*, Springer-Verlag, Berlin, 1962.
- [11] M. HIROYUKI, E. C. GARTLAND, JR., J. R. KELLY, AND J. PHILIP, *Multidimensional director modeling using the Q tensor representation in a liquid crystal cell and its application to the π cell with patterned electrodes*, Japan. J. Appl. Phys., 38 (1999), pp. 135–146.
- [12] R. JAMES, E. WILLMAN, F. A. FERNÁNDEZ, AND S. E. DAY, *Finite-element modeling of liquid-crystal hydrodynamics with a variable degree of order*, IEEE Trans. Electron Devices, 53 (2006), pp. 1575–1582.
- [13] J. KATRIEL, G. F. KVENTSEL, G. R. LUCKHURST, AND T. J. SLUCKIN, *Free energies in the Landau and molecular field approaches*, Liq. Cryst., 1 (1986), pp. 337–355.
- [14] I.-C. KHOO, *Liquid Crystals*, Wiley Ser. Pure Appl. Optics, John Wiley, Hoboken, NJ, 2007.
- [15] L. LONGA, D. MONSELESAN, AND H. R. TREBIN, *An extension of the Landau-Ginzburg-de Gennes theory for liquid crystals*, Liq. Cryst., 2 (1987), pp. 769–796.
- [16] L. LONGA AND H. R. TREBIN, *Integrity basis approach to the elastic free energy functional of liquid crystals*, Liq. Cryst., 5 (1989), pp. 617–622.
- [17] A. MAJUMDAR, *Equilibrium order parameters of liquid crystals in the Landau-De Gennes theory*, European J. Appl. Math., 21 (2010), pp. 181–203.
- [18] S. MKADDEM AND E. C. GARTLAND, *Fine structure of defects in radial nematic droplets*, Phys. Rev. E, 62 (2000), pp. 6694–6705.
- [19] N. MUKOZHAKA, N. YOSHIDA, H. TOYODA, Y. KOBAYASHI, AND T. HARA, *Diffraction efficiency analysis of a parallel-aligned nematic-liquid-crystal spatial light modulator*, Appl. Opt., 33 (1994), pp. 2804–2811.
- [20] C. W. OSEEN, *The theory of liquid crystals*, Trans. Faraday Soc., 29 (1933), pp. 883–899.
- [21] A. SIGNORINI, *Sulle deformazioni termoelastiche finite*, in Proceedings 3rd International Congress for Applied Mechanics, Vol. 2, 1930, pp. 80–89.
- [22] A. SONNET, A. KILLIAN, AND S. HESS, *Alignment tensor versus director: Description of defects in nematic liquid crystals*, Phys. Rev. E, 52 (1995), pp. 718–722.
- [23] J. F. THOMPSON, Z. U. A. WARSİ, AND C. W. MASTIN, *Numerical Grid Generation: Foundations and Applications*, North-Holland, Amsterdam, 1985.
- [24] L. N. TREFETHEN, *Spectral Methods in MATLAB*, SIAM, Philadelphia, 2000.
- [25] G. V. PRAKASH, M. KACZMAREK, A. DYADYUSHA, J. J. BAUMBERG, AND G. D'ALESSANDRO, *Control of topological defects in microstructured liquid crystal cells*, Opt. Express, 13 (2005), pp. 2201–2209.
- [26] Y. H. WAN AND J. E. MARSDEN, *Symmetry and bifurcation in three-dimensional elasticity. III. Stressed reference configurations*, Arch. Rational Mech. Anal., 84 (1983), pp. 203–233.
- [27] E. WILLMAN, F. A. FERNANDEZ, R. JAMES, AND S. E. DAY, *Modeling of weak anisotropic anchoring of nematic liquid crystals in the Landau-de Gennes theory*, IEEE Trans. Electron Devices, 54 (2007), pp. 2630–2637.